New Journal of Physics
The open access journal at the forefront of physics

Deutsche Physikalische Gesellschaft DPG IOP Institute of Physics

PAPER • OPEN ACCESS

Levitated optomechanics with a fiber Fabry–Perot interferometer

To cite this article: A Pontin *et al* 2018 *New J. Phys.* **20** 023017

IOP Publishing New J. Phys. 20 (2018) 023017 https://doi.org/10.1088/1367-2630/aaa71c

New Journal of Physics
The open access journal at the forefront of physics

Deutsche Physikalische Gesellschaft DPG
IOP Institute of Physics

Published in partnership with: Deutsche Physikalische Gesellschaft and the Institute of Physics

OPEN ACCESS

RECEIVED
20 September 2017

REVISED
13 November 2017

ACCEPTED FOR PUBLICATION
12 January 2018

PUBLISHED
7 February 2018

PAPER

Levitated optomechanics with a fiber Fabry–Perot interferometer

A Pontin[1], L S Mourounas[1], A A Geraci[2] and P F Barker[1]

[1] Physics Department, University College London, London, United Kingdom
[2] Physics Department, University of Nevada, Reno, NV, United States of America

E-mail: a.pontin@ucl.ac.uk

Keywords: levitated optomechanics, fiber interferometer, optical cooling

Abstract

In recent years, quantum phenomena have been experimentally demonstrated on variety of optomechanical systems ranging from micro-oscillators to photonic crystals. Since single photon couplings are quite small, most experimental approaches rely on the realization of high finesse Fabry–Perot cavities in order to enhance the effective coupling. Here we show that by exploiting a, long path, low finesse fiber Fabry–Perot interferometer ground state cooling can be achieved. We model a 100 m long cavity with a finesse of 10 and analyze the impact of additional noise sources arising from the fiber. As a mechanical oscillator we consider a levitated microdisk but the same approach could be applied to other optomechanical systems.

Cavity optomechanics [1] has achieved several long-awaited experimental results highlighting the quantum nature of the interaction. From the generation of ponderomotive squeezing [2–4] and field quadrature QND measurement [5] to the cooling of the mechanical motion to a thermal occupation number below unity [6–9]. These results, obtained in a variety of systems, have increased the interest in the generation of other non-classical states and in the investigation of the quantum to classical transition. In recent years, optical cooling of levitated dielectric nanoparticles [10] has been receiving a lot of attention. These unclamped oscillators offer the possibility to be operated in a regime where thermal noise, due to the residual background gas, is not the main contribution to the overall decoherence rate. Typically, the nanoparticle is trapped by optical tweezers [11] or an electro-dynamic [12] trap and cooled by an optical cavity field. In these configurations random momentum kicks to the nanoparticle associated with radiation pressure shot noise represent a major limitation toward ground state cooling, as has been recently reported [13].

An intriguing possibility towards the suppression of recoil heating is to levitate an apodized microdisk. If its radius is significantly bigger than the optical waist a microdisk behaves as a thin dielectric slab for which scattering occurs only due to surface roughness. This is in stark contrast to a sub-wavelength nanosphere that scatters light in a dipole field pattern. A similar system was initially proposed in [14], where a tethered microdisk was considered. They showed that by apodizing the edges of the microdisk even for a radius comparable to the waist, the scattering limited finesse is $\gg 10^4$.

Most optomechanical systems require a high finesse optical cavity in order to enhance the light–matter interaction. Here, we propose a levitated microdisk trapped in the standing wave of a long low finesse extrinsic fiber Fabry–Perot (FFP) interferometer. This scheme is shown in figure 1. The input field is injected into the cavity via an input coupler with a small radius of curvature, the field is propagated in free space for a few millimeters and then coupled into a single mode fiber. At the far end of the fiber a high reflectivity mirror or a distributed Bragg reflector provides the end mirror for the FFP.

There are three critical aspects that need to be addressed. These include the optical losses that are introduced at the fiber/free space interface, the cavity mode volume that will determine the microdisk coupling to the optical fields and the additional noise sources and nonlinear effects introduced by the fiber that could hinder the overall performance of the system.

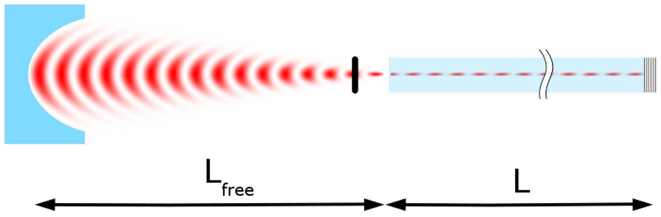

Figure 1. Scheme of the FFP interferometer. The optical cavity is divided in two parts: a free space region, $L_{\rm free}$, where the microdisk is trapped and an optical fiber, of length L. The optical mode transitions from a guided HE11 mode to a Gaussian mode. A dielectric microdisk, marked as dark thick line, is optically trapped in an antinode of the cavity standing wave close to the fiber output.

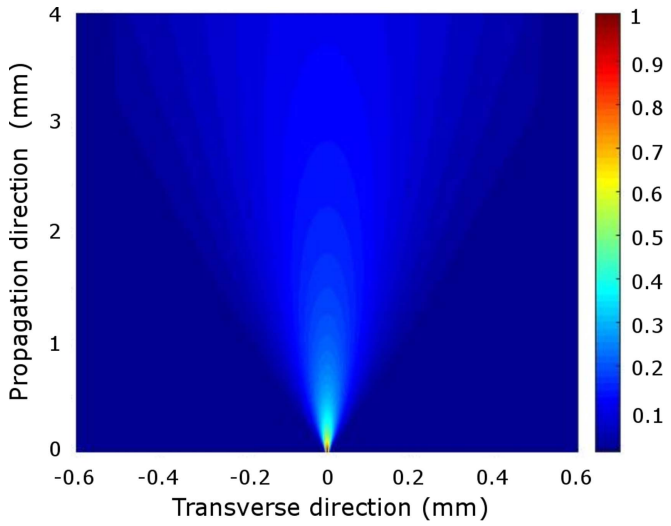

Figure 2. Intensity distribution of the initial HE11 mode as it propagates in free space.

Optical losses and move volume

Optical losses have been evaluated with numerical methods aimed at calculating the cavity reflection coefficient (considering ideal input and output couplers). The beam propagates from the fiber tip into free space using a finite difference beam propagation method [15]. The initial field profile is assumed to be the fundamental HE11 guided mode of the fiber. After a length $L_{\rm free}$ the beam is reflected by a mirror and propagates back to the fiber. The beam is propagated through 1 mm of fiber via the propagation method [16] after which the field is very well approximated by the HE11 mode. The total round trip power loss is obtained by comparing the initial and final power. The parameters considered are $L_{\rm free} = 4$ mm, a field of wavelength of $\lambda = 1550$ nm propagating through a Corning SMF-28 optical fiber. With these values an overall power loss of 4.13% was calculated, corresponding to an interface limited cavity finesse of $\mathcal{F} \simeq 150$. An example of the intensity profile obtained before reflection in shown in figure 2.

The cavity mode volume is defined as

$$V_m = \int |E(\mathbf{r})|^2 \mathrm{d}V, \tag{1}$$

where $E(\mathbf{r})$ is the normalized cavity field. We divide the integral in two domains, fiber and free space. In the former $E(\mathbf{r}) = \cos(kz)\mathrm{Exp}(-r^2/w_o^2)$, where $k = 2\pi/\lambda$ and w_o is the fiber mode-field radius (mfr), while in the trapping region

$$E(\mathbf{r}) = \cos(kz)\frac{\mathrm{Exp}(-r^2/w^2(z))}{\sqrt{1 + (z/z_{\rm R})^2}} \tag{2}$$

with $w(z) = w_o\sqrt{1 + (z/z_{\rm R})^2}$, and $z_{\rm R}$ is the Rayleigh range. Equation (2) neglects the curvature of the wavefronts and the details of the mirror geometry. However, for the parameters considered in the following the para axial approximation holds [17] and the contribution to the total mode volume coming from the free space region is only of the order of a few % and thus equation (2) provides a good estimate. By evaluating the integral in equation (1) we find

$$V_m = \frac{\pi w_o^2 n_s L}{4}\left(1 + \frac{L_{\text{free}}}{n_s L}\right), \tag{3}$$

where L_{free} is the length of the free space region, L is the fiber length and n_s its refractive index. A fiber cavity allow us a cavity waist of the order of the wavelength without the need to work with a near concentric configuration which is close to instability [18].

Fiber noises and nonlinear effects

We are going to assume that the environmental, electronic and classical laser noises can be controlled to a negligible level, such that, the fundamental noise introduced by the fiber is thermoptic induced phase noise. This is usually referred to as thermal phase noise in the fiber community. Since the intensities required for trapping the microdisk are typically rather high, nonlinear effects like Brillouin and Raman scattering must be considered.

Fiber thermal noise

Fiber interferometers, in various configurations (such as Mach–Zehnder and Michelson), constitute an active field of research especially for sensing applications [19]. The current generation of devices are approaching the fundamental thermal noise limit. This has been measured with high accuracy in a Mach–Zehnder interferometer [20] and compared to a model initially proposed by Wanser [21]. In his theory, the power spectral density (PSD) of phase noise for a fiber of length L can be estimated to be [22]

$$S_{\phi\phi}(\omega) = \pi \frac{L k_B T^2}{\kappa_t}\left(\frac{n_s q}{\lambda}\right)^2 F(\omega), \tag{4}$$

where $q = \alpha_L + \frac{1}{n_s}\frac{\mathrm{d}n_s}{\mathrm{d}T}$ is the thermoptic coefficient, α_L the linear expansion coefficient, κ_t is the thermal conductivity of the fiber medium and $F(\omega)$ is a term that characterizes a frequency cut-off dependent on fiber geometry. This is given by:

$$F(\omega) = \ln\left(\frac{k_{\text{max}}^4 + (\omega/D)^2}{k_{\text{min}}^4 + (\omega/D)^2}\right). \tag{5}$$

In this expression $k_{\text{max}} = 2/w_o$, $k_{\text{min}} = 2.405/a_f$, where a_f is the fiber outer radius, and D is the thermal diffusivity. Equation (4) describes the variance of the phase after the light field as passed through the fiber once. In the FFP the light bounces multiple times between the cavity mirrors so that the final total phase noise grows with an increasing finesse. In order to include thermal phase noise in the cavity dynamical equations it is simple to consider it as a detuning noise, that is $S_{\dot{\phi}\dot{\phi}}(\omega) = (c/2n_s L)^2 S_{\phi\phi}(\omega)$, where c is the speed of light.

Raman and Brillouin Scattering

For an optical field propagating in a molecular medium a fraction of the total power can be transferred to a frequency downshifted field through the interaction with the vibrational modes of the medium. Acoustic phonons are involved in Brillouin scattering while optical phonons participate in Raman scattering. For both processes the nonlinear dynamics becomes exponentially more relevant after a critical threshold is surpassed. In the case of Raman scattering the critical power can be estimated as [23] $P_{\text{cr}} \approx \frac{16 A_{\text{eff}}}{g_R L}$ where L is the fiber length, $A_{\text{eff}} = \pi w_o^2$ is the effective mode area and $g_R \simeq 6.4 \times 10^{-14}$ m W^{-1} is the peak Raman gain. A typical value for the mode-field radius at 1550 nm is 5.25 μm and considering a 100 m long fiber, then $P_{\text{cr}} = 216$ W. A similar expression can be exploited for the case of Brillouin scattering [23] where $P_{\text{cr}} \approx \frac{21 A_{\text{eff}}}{g_B L}$, and $g_B \simeq 5 \times 10^{-11}$ m W^{-1} is the typical peak brillouin gain for step index silica fibers. For the parameters considered before we obtain $P_{\text{cr}} \simeq 350$ mW. As for the case of phase noise, these values correspond to a single pass through the fiber. For a FFP the thresholds can be significantly reduced [24, 25]. However, lower values for g_B have been reported in the literature [26]. Furthermore, stimulated Brillouin scattering is one of the most important limiting factors in high power fiber lasers and, as such, increasing its threshold is a highly researched topic. The mainstream approach relies on the introduction of non-uniformities in the fiber to achieve spectral broadening of the Brillouin gain spectrum, thus reducing the peak value g_B. These non-uniformities ranges from temperature gradients [27] to modifications of fiber composition or geometry [28, 29].

Description of the model

We consider an apodized microdisk, of radius a and thickness t, trapped in the standing wave of the FFP within 1–2 Rayleigh ranges from the fiber/free-space interface. This correspond to a distance between 60 and 120 μm.

We assume a high aspect ratio $a/t > w_o/\lambda$ in order to minimize both modifications of the Gaussian profile and scattering of the intra-cavity field. More details on the effects of the apodization and of the aspect ratio can be found in [14]. We focus on the center-of-mass degree of freedom of the microdisk along the cavity axis. The transverse confinement is typically weaker giving much lower dynamical timescales while the lowest flexural mode typically has a frequency $\gg$1 MHz. Three beams drive the cavity: a high power trapping beam at $\lambda_{\rm trap}$ and two low power beams at $\lambda_{\rm cm} \simeq \lambda_{\rm trap} \equiv \lambda$ to cool and detect the microdisk motion. The model we are considering is, thus, an extension of that presented in [30]. We add to that description an additional field and include the fiber phase noise contribution. It must be pointed out that this treatment is based on the high finesse approximation, that is, describing the optical resonance as a Lorentzian. For the finesse values that we are going to consider the difference with the Airy peak and a Lorentzian can be significant amounting to a 30% increase in linewidth and a decrease of intra-cavity power by a similar amount. The equation of motions are:

$$\begin{aligned}\dot{a}_i &= -[\kappa - \mathrm{i}(\Delta_o^i + \dot{\phi}_i)]\, a_i + \mathrm{i}g_o a_i \cos^2(kx - \phi_i) \\ &\quad + \sqrt{2\kappa_{\rm in}}\ \alpha_{{\rm in},i} + \nu_i, \\ \ddot{x} &= \frac{\xi}{m} - \gamma_g \dot{x} - \frac{\hbar k g_o}{m}\sum_i a_i^\dagger a_i \sin[2(kx - \phi_i)],\end{aligned} \tag{6}$$

where $i = t, c, m$ meaning trap, cooling and meter fields which is a weak resonant field that is exploited for measurement purposes. In equations (6) $g_o = \frac{V_d}{2V_m}(\epsilon - 1)\omega_l$ is the coupling strength, ω_l is the field frequency, Δ_o^i is the empty cavity detuning, $\kappa = \kappa_{\rm in} + \kappa_{\rm out} + \kappa_{\rm loss}$ is the total cavity half-linewidth, $\alpha_{{\rm in},i}$ is the driving amplitude, $\nu_i = \sqrt{2\kappa_{\rm in}}\ a_{{\rm in},i} + \sqrt{2\kappa_{\rm out}}\ a_{{\rm out},i} + \sqrt{2\kappa_{\rm loss}}\ a_{{\rm loss},i}$ is a weighted sum of all vacuum operators and $\dot{\phi}_i$ is a detuning noise term that accounts for the fiber phase noise. This is considered to provide an uncorrelated contribution to all cavity fields, that is $\langle \dot{\phi}_i(t)\dot{\phi}_j(t')\rangle = 0$. The field fluctuations are uncorrelated and have the following correlation functions [31]

$$\begin{aligned}&\langle a_i(t)a_j(t')\rangle = \langle a_i^\dagger(t)a_j^\dagger(t')\rangle = \langle a_i^\dagger(t)a_j(t')\rangle = 0 \\ &\langle a_i(t)a_j^\dagger(t')\rangle = \delta(t - t').\end{aligned} \tag{7}$$

Finally, ξ is a Brownian stochastic force with zero mean value that arises from the background gas and obeying the correlation function [31, 32]:

$$\langle \xi(t)\xi(t')\rangle = \frac{\gamma_g}{\omega_t}\int \frac{\mathrm{d}\omega}{2\pi}\mathrm{e}^{-\mathrm{i}\omega(t-t')}\omega\left[\coth\left(\frac{\hbar\omega}{2k_{\rm B}T}\right) + 1\right], \tag{8}$$

where $k_{\rm B}$ is the Boltzman constant and γ_g is the viscous damping rate.

We consider $\alpha_{{\rm in},c} = R_1\ \alpha_{{\rm in},t}$ and $\alpha_{{\rm in},m} = R_2\ \alpha_{{\rm in},t}$ with $0 < R_1, R_2 \leqslant 1$. The steady state is readily obtained to be

$$\begin{aligned}\alpha_i &= \frac{\sqrt{2\kappa_{\rm in}}}{\kappa - \mathrm{i}\,\Delta^i}\ \alpha_{{\rm in},i}, \\ -\frac{\sin[2(kx_o - \phi_1)]}{\sin[2(kx_o - \phi_2)]} &= \frac{(1 + \delta_t^2)}{(1 + \delta_c^2)(1 + \delta_m^2)} \\ &\quad \times [R_1^2(1 + \delta_m^2) + R_2^2(1 + \delta_c^2)],\end{aligned} \tag{9}$$

where Δ_i is the hot cavity detuning and $\delta_i = \Delta_i/\kappa$. Upon displacement of the operators in equations (6) and subsequent linearization the dynamical equations become

$$\begin{aligned}\dot{a}_i &= -(\kappa - \mathrm{i}\Delta_i)\, a_i - \mathrm{i}g_o k\alpha_i \sin[2(kx_o - \phi_i)]\, x - \mathrm{i}\alpha_i\dot{\phi} + \nu_i, \\ \ddot{x} &= -\omega_t^2 x - \frac{\hbar k g_o}{m}\sum_i (a_i^\dagger\ \alpha_i + a_i\ \alpha_i^*)\sin[2(kx_o - \phi_i)] \\ &\quad - \gamma_g\dot{x} + \xi/m,\end{aligned} \tag{10}$$

where $\omega_t^2 = \frac{2\hbar k^2 g_o}{m}\sum_i(|\alpha_i|^2\cos[2(kx_o + \phi_i)])$ is the optical trap frequency. In the following we will assume $\phi_1 = 0$, $\phi_2 = \pi/4$, $R_1, R_2 \ll 1$ and $\Delta_t = \Delta_m = 0$ so that $x_o \simeq 0$ represents a good approximation considerably simplifying the model since the effective optomechanical parameters are purely determined by the cooling field. Thus, by moving into Fourier space and defining

$$A_{i,\pm}(\omega) = \frac{\hbar k^2 g_o^2 |\alpha_i|^2}{m\omega} \frac{\kappa}{\kappa^2 + (\omega \mp \Delta_i)^2} \tag{11}$$

with which the effective mechanical parameters can be expressed as $\gamma_{\rm eff} = \gamma_m + \gamma_{\rm opt} = \gamma_m + A_{c,-} - A_{c,+}$ and[3] $\omega_{\rm eff}^2 = \omega_t^2 + \frac{\omega}{\kappa}[(\Delta_c + \omega)\, A_{c,-} + (\Delta_c - \omega)\, A_{c,+}]$, the mechanical susceptibility is $\chi_{\rm eff}(\omega) = [m\,(\omega_{\rm eff}^2 - \omega^2 - {\rm i}\omega\gamma_{\rm eff})]^{-1}$. The symmetrized displacement PSD, then, is given by

$$\frac{\bar{S}_{xx}(\omega)}{|\chi_{\rm eff}(\omega)|^2} = S_{\rm th} + \sum_i [\hbar m\omega\, (A_{i,+} + A_{i,-})] + \sum_i 4\Delta_i^2 \frac{m^2\omega^2}{g_o^2 k^2 \kappa^2} A_{i,+}\, A_{i,-}\, S_{\dot\phi\dot\phi}(\omega). \tag{12}$$

Equation (12) accounts for all force noises acting on the microdisk except for recoil heating due to the trapping potential. This can be included through the substitution $S_{\rm th} \to S_{\rm th}\,(1 + \gamma_{\rm sc}/\bar{n}\gamma_g)$, where $\bar{n} = k_{\rm B}T/\hbar\omega_t$ is the initial phonon number and $\gamma_{\rm sc} = \frac{V_m}{V_d}\frac{\lambda}{4L}\frac{\omega_t}{(\epsilon-1)\mathcal{F}_{\rm disk}}$ is the recoil heating rate in which $\mathcal{F}_{\rm disk} \simeq 10^5$ is the disk-limited cavity finesse [14]. By assuming $\omega_t \gg \bar{n}\gamma_g$, g_i and $\kappa \gg \gamma_g$, g_i, where and $g_i = g_o k\sqrt{\hbar/m\omega_t}\,|\alpha_i|$ is the effective coupling strength, the final phonon occupation number is given by [33]

$$n_f = \frac{\bar{n}\gamma_g + \gamma_{\rm sc} + \sum_i [A_{i,+} + 2\Delta_i^2 \frac{m\omega_t}{\hbar g_o^2 k^2 \kappa^2} A_{i,+} A_{i,-} S_{\dot\phi\dot\phi}(\omega_t)]}{\gamma_{\rm eff}}. \tag{13}$$

It is possible to exploit equation (13) to estimate a maximum injected cooling power before the fiber phase noise starts contributing significantly.

Phase noise introduced by the fiber can have a significant impact on detection sensitivity since it could increase the detection noise floor. This can be evaluated by looking at the homodyne PSD of the resonant meter field. By using equation (10) and by defining $K_i(\omega) = [\kappa - {\rm i}(\omega + \Delta_i)]^{-1}$ and $G(\omega) = {\rm i}\hbar g_o^2 k^2 K_m(\omega)\chi_{\rm eff}(\omega)$ we can express the intra-cavity meter field as

$$\begin{aligned} a_m = {} & v_m\, K_m(\omega)[1 + |\alpha_m|^2 G(\omega)] + v_m^\dagger [\alpha_m^2 K_m^*(-\omega) G(\omega)] \\ & + v_c [\alpha_m \alpha_c^* K_c(\omega) G(\omega)] + v_c^\dagger [\alpha_m \alpha_c K_c^*(-\omega) G(\omega)] \\ & + \dot\phi_m\, \alpha_m \{{\rm i}K_m(\omega) - {\rm i}G(\omega)|\alpha_m|^2 [K_m(\omega) - K_m^*(-\omega)]\} \\ & + \dot\phi_c \{-{\rm i}G(\omega)\alpha_m |\alpha_c|^2 [K_c(\omega) - K_c^*(-\omega)]\} \\ & + {\rm i}g_o k \alpha_m K_b(\omega)\chi_{\rm eff}(\omega)\, \xi. \end{aligned} \tag{14}$$

By using standard input–output formalism the reflected meter field is given by $b_{\rm out} = -a_{{\rm in},m} + \sqrt{2\kappa_{\rm in}}\, a_m$; than as usual the homodyne observable is defined as $\mu = b_{\rm out}\, {\rm e}^{-{\rm i}\theta} + b_{\rm out}^\dagger\, {\rm e}^{{\rm i}\theta}$.

Results

We consider a FFP whose input coupler is held at $L_{\rm free} = 4$ mm from the fiber input face and a 100 m long fiber at the end of which an ideal mirror is assumed. The fiber has a core (cladding) diameter of 8.7 (125) μm and a mfr = 5.25 μm. The system is considered to be held in a UHV environment at a pressure $P = 10^{-9}$ mbar which corresponds to a gas-damping coefficient $\gamma_g = 32P/\pi\bar{v}\rho t$. The cavity finesse is $\mathcal{F} = 10$, which gives a FSR = 1 MHz and a cavity half-linewidth $\kappa/2\pi = 51$ kHz, optical losses introduced by the fiber-free space interface contribute to the overall decay channel by ~7%. The apodized microdisk has a radius of 8 μm and a thickness $t = 0.5$ μm. With these values the coupling parameter is $g_o/2\pi = 3$ MHz. The trapping frequency is chosen to be $\omega_t/2\pi = 10^5$ Hz which is achieved with a trapping beam power of $P_t = 60$ mW. The trapping depth for the parameters chosen is approximately 2×10^8 K. An estimate of the optimal cooling beam power can be obtained using equation (13) by requiring that the phase noise contribution equals the cooling beam back-action. That is, we impose $2\Delta_i^2 \frac{m\omega_t}{\hbar g_o^2 k^2} A_{c,-} S_{\dot\phi\dot\phi}(\omega_t) = 1$. Assuming a detuning of $\Delta_c = -\omega_t$ and a ratio $r = \omega_t/\kappa$ we find $P_c^{\rm max} \simeq \hbar\omega_l \frac{1+r^2}{4r^4}\frac{\omega_t^2}{S_{\dot\phi\dot\phi}(\omega_t)} = 12$ μW for our parameters. With these parameters the optical cooling rate $\gamma_{\rm opt}/2\pi = 300$ Hz ($Q_{\rm eff} \simeq 330$). We consider a meter beam power of $P_m = 4.3$ μW which provides a good compromise between final phonon number occupation and peak-to-noise ratio (PNR) in the homodyne detection. Despite the extremely low finesse a final thermal occupation number smaller than one can be obtained. This is shown in figure 3 where we plot the final effective phonon number n_f as a function of cooling field detuning δ_c. As imposed, fiber phase noise gives an equal contribution to the cooling field back-action. This occurs with a $S_{\phi\phi} \simeq 10^{-15}$ rad^2 Hz^{-1} at the trap frequency. The limiting contribution comes from the back-

[3] To simplify the notation we use $A_{i,\pm} \equiv A_{i,\pm}(\omega_t)$.

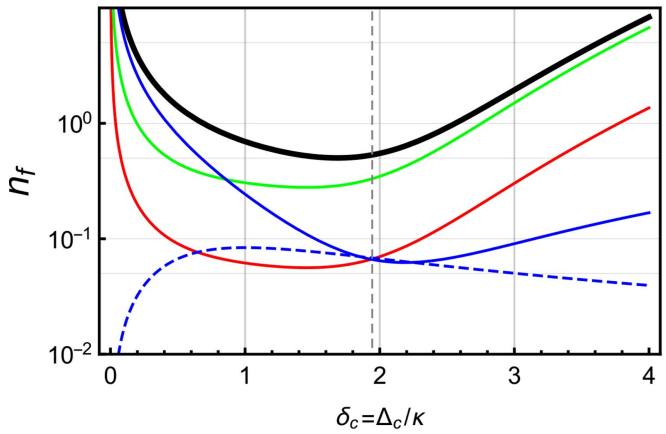

Figure 3. Expected final phonon number as function of the cooling field normalized detuning. All contributions are shown: total (black), thermal noise (red), cooling field back-action (blue), meter field back-action (green) and fiber phase noise contribution (dashed-blue). The vertical dashed-gray line indicates the detuning $\Delta_c = \omega_t$ that maximizes the cooling rate in the resolved sideband regime.

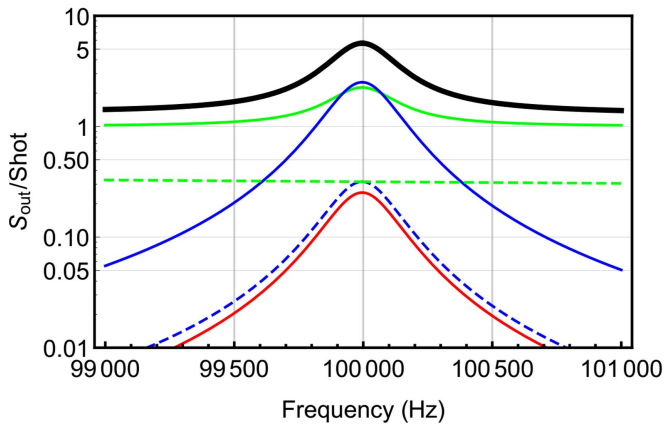

Figure 4. Phase quadrature homodyne spectra of the meter field normalize to shot noise. All contributions are shown: total (black), thermal noise (red), cooling field back-action (blue), meter field back-action (green), fiber phase noise contribution for the meter field (dashed-green) and fiber phase noise contribution for the cooling field (dashed-blue).

action of the meter. A direct consequence is that the minimal n_f is no longer obtained for the typical optimal detuning in the resolved sideband regime but at a slightly lower value. This is found to be $\delta_c = -0.87\ \omega_t$ for which a $n_f = 0.5$ is obtained. Interestingly, without the meter field back-action the final phonon number would be $n_f = 0.17$ despite the contribution from the fiber phase noise.

To verify the detectability of the microdisk motion we evaluated the homodyne spectra of the phase quadrature for the resonant meter field. This is show in figure 4 where we plot the total quadrature PSD normalized to shot noise along with all contributions. The dominant noise floor is given by the meter field shot noise with a non-negligible contribution due to fiber phase noise. We point out that this is the case since the trapping frequency for the microdisk is significantly higher than the frequency cut-off described by equation (5). Indeed, phase noise contribution is orders of magnitude higher at low frequency.

In order to emphasize the tradeoff between detectability and final occupation number, we show in figure 5 a contour plot of n_f as function of cooling beam detuning Δ_c and achievable PNR. A final $n_f = 1$ can be obtained with a high PNR $= 25$ with an input power of $P_m = 12.3\ \mu$W. Interestingly, n_f has a smooth dependance on Δ_c since the system is not deeply into the resolved sideband regime.

In conclusion, we have shown that an apodized microdisk trapped in an extrinsic FFP interferometer could be cooled down to the quantum ground state despite the extremely low finesse of the system. Thermoptic phase noise introduced by random temperature fluctuations along the fiber has been taken into account and has been shown not to constitute an intrinsic limit toward ground state cooling. Further analysis is however required. The intra-cavity power of the trapping beam is ~360 mW, this value coincides with the threshold for Brillouin scattering for a single pass in the 100 m long fiber considered here. This implies that additional measures to

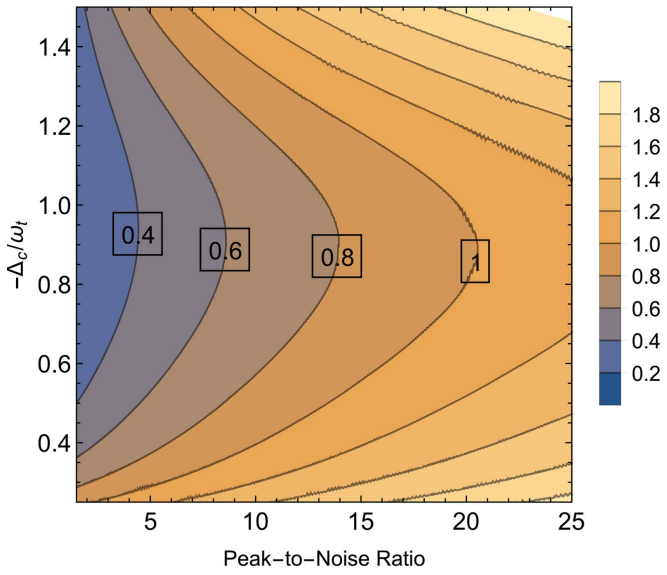

Figure 5. Contour plot of the achievable final thermal occupation number as a function of cooling beam detuning and achievable PNR.

significantly increase the Brillouin threshold need to be put in place. An intriguing possibility is the use of photonic crystal hollow-core fibers (HCF) which have an increased power handling capability thanks to a reduced interaction with silica [34]. At the same time, a lower thermal phase noise level has been measured for HCFs [35] allowing more flexibility in the parameters choice. Optical losses at the interface have already been estimated and found of the same order as for a standard single mode fiber, however, HCFs have significantly higher losses and coupling to higher modes could impact the system performance [35].

It has been recently proposed that a levitated sensor could be exploited to detect high frequency gravitational waves [36]. It has been shown that, under the right conditions, the attainable sensitivity could be more than an order of magnitude better than current interferometers like LIGO and VIRGO in the frequency range of 50–300 kHz. The configuration considered here could represent a viable alternative to implement such a proposal, and will be studied in future work, with the fiber-based cavity potentially eliminating the demand for large optical mirrors. A variety of sources could produce gravitational waves at such frequencies, including signals from black hole superradiance [37]. For example such signals can be associated with the QCD axion, a notable dark matter candidate [38]. Such sources can also be sought after in current advanced gravitational wave interferometer observatories [39], and the more compact levitated-sensor approach could significantly expand the search capabilities in the higher frequency band [36].

Acknowledgments

The authors acknowledge funding from the EPSRC Grant No. EP/N031105/1. AP has received funding from the European Unions Horizon 2020 research and innovation programme under the Marie Sklodowska-Curie Grant Agreement No. 749709. AG is supported by the US National Science Foundation grant no. PHY-1506431 and the Heising-Simons Foundation.

ORCID iDs

A Pontin https://orcid.org/0000-0002-9705-697X

References

[1] Aspelmeyer M, Kippenberg T and Marquardt F 2014 *Rev. Mod. Phys.* **86** 1391
[2] Brooks D W C *et al* 2012 *Nature* **488** 476
[3] Safavi-Naeni A H *et al* 2013 *Nature* **500** 185
[4] Purdy T P *et al* 2013 *Phys. Rev.* X **3** 031012
[5] Pontin A *et al* 2016 arXiv:1611.00917
[6] Connell A D *et al* 2010 *Nature* **464** 697
[7] Teufel J D *et al* 2011 *Nature* **475** 359

[8] Chan J et al 2011 Nature 478 89
[9] Underwood M et al 2015 Phys. Rev. A 92 031802
[10] Barker P F and Shneider M N 2010 Phys. Rev. A 81 023826
Chang D E et al 2010 Proc. Natl Acad. Sci. 107 1005
Romero-Isart O et al 2010 New J. Phys. 12 033015
[11] Li T et al 2011 Nat. Phys. 7 527
Gieseler J et al 2012 Phys. Rev. Lett. 109 103603
[12] Millen J et al 2015 Phys. Rev. Lett. 114 123602
[13] Jain V et al 2016 Phys. Rev. Lett. 116 243601
[14] Chang D E et al 2012 New J. Phys. 14 045002
[15] Chung Y and Dagli N 1990 IEEE J. Quantum Electron. 26 1335
[16] Feit M D and Fleck J A 1978 Appl. Opt. 17 3990
[17] Tey M K et al 2009 New J. Phys. 11 043011
[18] Durac K et al 2014 New J. Phys. 16 103002
[19] Kirkendall C K and Dandridge A 2004 J. Phys. D: Appl. Phys. 37 R197
[20] Bartolo R E et al 2012 IEEE J. Quantum Electron. 48 720
[21] Wanser K H 1992 Electron. Lett. 28 53
[22] Dong J, Huang J and Li T 2016 Appl. Phys. Lett. 108 021108
[23] Agrawal G 1995 Nonlinear Fiber Optics (New York: Academic)
[24] Ogusu K 2003 J. Opt. Soc. Am. B 20 685
[25] Labudde P et al 1980 Opt. Commun. 32 385
[26] Lanticq V et al 2009 Opt. Lett. 34 1018
[27] Kovalev V I and Harrison R G 2006 Opt. Lett. 31 161
[28] Kobyakov A 2005 Opt. Express. 13 5338
[29] Evert A et al 2012 Opt. Express. 20 17401
[30] Monteiro T 2013 New J. Phys. 15 015001
[31] Gardiner C W and Zoller P 2000 Quantum Noise (New York: Springer)
[32] Landau L D and Lifshitz E 1958 Statistical Physics (New York: Pergamon)
[33] Abdi M et al 2011 Phys. Rev. A 84 032325
[34] Ouzounov D G et al 2003 Science 31 1702
[35] Cranch G A and Miller G A 2015 Appl. Opt. 54 F8
[36] Arvanitaki A and Geraci A A 2013 Phys. Rev. Lett. 110 071105
[37] Arvanitaki A, Dimopoulos S, Dubovsky S, Kaloper N and March-Russell J 2010 Phys. Rev. D 81 123530
Arvanitaki A and Dubovsky S 2011 Phys. Rev. D 83 044026
[38] Arvanitaki A, Baryakhtar M and Huang X 2015 Phys. Rev. D 91 084011
[39] Arvanitaki A, Baryakhtar M, Dimopoulos S, Dubovsky S and Lasenby R 2017 Phys. Rev. D 95 043001